Biology of Reproduction, 2022, **106(6)**, 1312–1326
https://doi.org/10.1093/biolre/ioac057
Advance access publication date 16 March 2022
Research Article

Loss of mouse Y chromosome gene *Zfy1* and *Zfy2* leads to spermatogenesis impairment, sperm defects, and infertility

Yasuhiro Yamauchi[1,‡], Takafumi Matsumura[2,‡], Jackson Bakse[1], Hayden Holmlund[1], Genevieve Blanchet[1], Emmaelle Carrot[1], Masahito Ikawa[2] and Monika A. Ward[1,†,*]

[1]Institute for Biogenesis Research, John A. Burns School of Medicine, University of Hawaii, Honolulu, HI, USA
[2]Department of Experimental Genome Research, Research Institute for Microbial Diseases, Osaka University, Suita, Osaka, Japan

***Correspondence:** Institute for Biogenesis Research, John A. Burns School of Medicine, University of Hawaii, 1960 East-West Road, Honolulu, HI 96822, USA. Tel: +8089560779; E-mail: mward@hawaii.edu

[†]**Grant Support:** This material is based on work supported by National Institutes of Health (HD072380) and Hawaii Community Foundation (10CON-86294) to (M.A.W.).

[‡]Co-first authors.

Abstract

Using mice with Y chromosome deficiencies and supplementing *Zfy* transgenes, we, and others, have previously shown that the loss of Y chromosome *Zfy1* and *Zfy2* genes is associated with infertility and spermiogenic defects and that the addition of *Zfy* transgenes rescues these defects. In these past studies, the absence of *Zfy* was linked to the loss of other Y chromosome genes, which might have contributed to spermiogenic phenotypes. Here, we used CRISPR/Cas9 to specifically remove open reading frame of *Zfy1*, *Zfy2*, or both *Zfy1* and *Zfy2*, and generated *Zfy* knockout (KO) and double knockout (DKO) mice. *Zfy1* KO and *Zfy2* KO mice were both fertile, but the latter had decreased litters size and sperm number, and sperm headshape abnormalities. *Zfy* DKO males were infertile and displayed severe spermatogenesis defects. Postmeiotic arrest largely prevented production of sperm and the few sperm that were produced all displayed gross headshape abnormalities and structural defects within head and tail. Infertility of *Zfy* DKO mice could be overcome by injection of spermatids or sperm directly to oocytes, and the resulting male offspring had the same spermiogenic phenotype as their fathers. The study is the first describing detailed phenotypic characterization of mice with the complete *Zfy* gene loss. It provides evidence supporting that the presence of at least one *Zfy* homolog is essential for male fertility and development of normal sperm functional in unassisted fertilization. The data also show that while the loss of *Zfy1* is benign, the loss of *Zfy2* is mildly detrimental for spermatogenesis.

Summary Sentence
Mice with a complete loss of Y chromosome encoded *Zfy1* and *Zfy2* genes generated by CRISPR/Cas9-mediated open reading frame knockout are infertile and display severe spermatogenesis and sperm defects.

Keywords: male infertility, spermatogenesis, sperm, testis, Y chromosome, assisted reproduction, *Zfy*, CRISPR/Cas9

Background

The Y chromosome encoded zinc finger protein gene, *Zfy*, has once been in the center of attention as a potential candidate for a testis-determining factor [1–3]. When the attention went to another Y chromosome gene, *Sry* [4–6], *Zfy* was quickly forgotten, and it has taken more than two decades for it to re-emerge with newly ascribed spermiogenic roles. The mouse Y chromosome has two *Zfy* copies, *Zfy1* and *Zfy2*, both with potential to act as a transcription factor and with postnatal expression essentially restricted to spermatogenic cells [7–9]. Since its re-emergence in 2010, various pieces of evidence were reported supporting the role of *Zfy1* and *Zfy2* in male fertility. It has been shown that mouse *Zfy1* and *Zfy2* play spermatogenic quality functions during the pachytene stage of meiosis and during meiosis I (MI) by triggering the apoptotic elimination of spermatocytes [10, 11] and regulating meiotic sex chromosome inactivation (MSCI) [12]. Mouse *Zfy2* and, to a lesser extent, *Zfy1* were also shown to promote the second meiotic division [13]. This was associated with de novo transcription of these genes during an interphase between the meiotic divisions suggesting that the male-specific meiotic interphase serves to allow for meiosis II (MII) critical X and Y gene reactivation following sex chromosome silencing in meiotic prophase. In our earlier work, we have shown that mouse *Zfy2* promotes spermatid elongation [14, 15] and enhances the efficiency of round spermatid injection (ROSI) [15]. We also demonstrated that mouse *Zfy2* is the sole Y chromosome gene responsible for enabling round spermatids to transform into sperm in the context of limited Y chromosome content. Mice lacking Y chromosome but transgenic for two Y-derived genes, *Sry* driving sex determination and *Eif2s3y* initiating spermatogenesis, produce only round spermatids [16]. When *Zfy2* was added as a third transgene, the males produced sperm and yielded offspring after intracytoplasmic sperm injection (ICSI) [15].

All the findings mentioned beforehand and supportive of the spermiogenic roles played by *Zfy* genes were obtained using mice with severe Y chromosome deficiencies (i.e., with loss of several Y genes in addition to the loss of *Zfy*) and with the same mice but with the *Zfy* transgenes added. Thus, interpretation of findings required acknowledging that altered expression or loss of Y genes other than *Zfy* might have contributed to observed spermiogenic phenotypes. The ultimate demonstration of *Zfy* function requires gene-specific

Received: December 16, 2021. **Revised:** February 17, 2022. **Accepted:** March 11, 2022

knockout (KO). In 2017, CRISPR/Cas9 system was used to generate individual *Zfy1* and *Zfy2* KO as well as *Zfy1* and *Zfy2* double knockout (DKO) mice [17]. *Zfy1* KO mice did not display any significant phenotype changes, *Zfy2* KO mice showed increased morphological abnormalities and reduced fertility, and the DKO mice were infertile with abnormal sperm morphology, fertilization, and embryonic development failure, and altered expression of some genes important for sperm function. Although this study provided explicit evidence for the importance of the presence of *Zfy1* and *Zfy2* for male fertility, the authors targeted exon 4 of the *Zfy* genes, which is the only exon known to undergo splicing resulting in *Zfy* transcript variants [18]. Thus, the targeting strategy has not assured that the KO was complete raising the possibility that partial ZFY1 and ZFY2 peptides were produced by these mice; a weakness was acknowledged by the authors.

Here, we report on generation and characterization of knockout mice, *Zfy1* (*Zfy1* KO), *Zfy2* (*Zfy2* KO), and *Zfy1* and *Zfy2* (*Zfy* DKO), with the entire coding regions of these genes deleted. Our results extend the previous data and provide new evidence regarding the effects of *Zfy* loss. The phenotypic characterization of KO and DKO males revealed that single-gene KO is compatible with male fertility, but with *Zfy2* KO, and not *Zfy1* KO males, displaying less efficient reproduction, and decreased sperm number and sperm quality. The loss of both *Zfy1* and *Zfy2* resulted in complete infertility, impairment in spermatogenesis progression regarding both numbers and quality of developing spermatids and sperm, and in some cases full postmeiotic arrest at the round spermatid stage. The presence of at least one *Zfy* homolog is thus critical for sperm formation, and the loss of both *Zfy* genes is detrimental to male fertility. Also, of the two homologues, *Zfy2* seems to be more important for normal spermatogenesis.

Materials and methods

Animals

The mice were used for breeding, generation of embryos for ES injections, fecundity testing, as vasectomized males and surrogate/foster females for embryo transfer, and as oocyte and sperm donors for assisted reproduction. Two strains, bred in-house, were used, CD-1 (originated from Charles River Laboratories Crl:CD-1(ICR); strain code: 022) and C57BL/6/J (originated from Jackson Laboratory, strain code: 000664).

The mice were fed ad libitum with a standard diet and maintained in a temperature- and light-controlled room (22°C, 14 h light/10 h dark), in accordance with the guidelines of the Laboratory Animal Services at the University of Hawaii and guidelines presented in National Research Council's (NCR) "Guide for Care and Use of Laboratory Animals" published by the Institute for Laboratory Animal Research (ILAR) of the National Academy of Science, Bethesda, MD, 2011. The protocol for animal handling and treatment procedures was reviewed and approved by the Animal Care and Use Committee at the University of Hawaii (animal protocol number 06-010).

The mice of interest in this study were males lacking the Y chromosome gene *Zfy1*, *Zfy2*, and both *Zfy1* and *Zfy2* that were produced by CRISPR/Cas9-mediated targeting leading to either single-gene KO or DKO. The KO and DKO mice were propagated by breeding or assisted fertilization and subjected to phenotype characterization.

Chemicals

Pregnant mares' serum gonadotrophin (eCG) and human chorionic gonadotrophin (hCG) were purchased from ProSpec, East Brunswick, NJ (HOR-272 and HOR-250). Other chemicals were obtained from Sigma Chemical Co. (St Louis, MO) unless otherwise stated.

Production of *Zfy1* KO mice

Our initial strategy to generate *Zfy* KO mice was to create chimeric mice via ESC gene targeting. While we succeed in obtaining *Zfy2* KO and *Zfy* DKO mice with this approach, we were unable to produce *Zfy1* KO males. Therefore, *Zfy1* KO mice were produced by electroporation of C57BL/6 zygotes. The gRNA/Cas9 ribonucleoprotein (RNP) was prepared as described previously (30 ng/μL gRNA, 70 ng/μL CAS9) [19] to remove the entire open reading frame (ORF) of the *Zfy1* gene. Two guide RNAs were designed using CRISPRdirect software (https://crispr.Dbcls.jp/) [20] (Supplementary Table S1). Two RNPs were combined and electroporated into the fertilized eggs using NEPA21 (NEPAGENE, Chiba, Japan) [resistance value: 550 ~ 600 Ω, poring pulse: 225 V (voltage), 2 ms (pulse amplitude), 50 ms (pulse interval), four (pulse number), 10% (attenuation), +(polarity), transfer pulse: 20 V (voltage), 50 ms (pulse amplitude), 50 ms (pulse interval), ±5 (pulse number), 40% (attenuation), +/− (polarity)] and the embryos were then transferred into pseudopregnant surrogate mothers. F0 founders were screened for successful targeting using PCR and sequencing and those positive provided sperm for ICSI to generate F1 *Zfy1* KO males. The loss of *Zfy1* was confirmed in F1 progeny by sequencing and transcript expression analysis. The F1 males, on pure C57BL/6 genetic background, were used for phenotype characterization.

Construction of *Zfy1* and *Zfy2* gene disruption vectors and production of targeted ES cells

To target *Zfy2*, two pX459 plasmids (Addgene #62988) were constructed to remove ORF of the *Zfy2* gene. Two guide RNAs were designed using CRISPRdirect software (https://crispr.Dbcls.jp/) [20] (Supplementary Table S1). The pX459 plasmids were transfected into EGR-G01 [129S2 x (*cag/acr-EGFP*)C57BL/6 N F1; B6/129 genetic background)] ESC [21] using Lipofectamine LTX & PLUS reagent (Thermo Fisher Scientific, A1261, Waltham, MA, USA [22]. The EGR-G01 ESCs were developed before from a transgenic mouse line expressing GFP both throughout the body from the transgene *CAG-EGFP* [23] and in the sperm acrosome from the transgene *Acr-EGFP* [24]. Targeted ESC clones were isolated by positive/negative selection with puromycin. Correct targeting of the *Zfy2* in ESC clones was determined by PCR analysis using primers shown in Supplementary Table S2.

For *Zfy2* KO, 3 out of 48 (6%) examined ESC clones (1C, 3B, and 4H) were shown to be successfully targeted with a deletion removing the entire *Zfy2* ORF by PCR analysis followed by sequencing. Within each clone, the majority of cells had a normal chromosome count at passage 16, with 100, 70, and 90% of examined cells having 40 chromosomes, for 1C, 3B, and 4H, respectively. The ESCs were used to make chimeric F0 founders.

To target both *Zfy2* and *Zfy1*, new pX459 plasmids were constructed to remove the entire ORF of *Zfy1*. These plasmids were transfected into ESCs that have already been successfully

targeted for *Zfy2*. Three *Zfy2* null ESC clones (1C, 3B, and 4H) were targeted to delete *Zfy1* and six DKO ESC clones were obtained (3C-1C, 2C-3B, 2H-3B, 3E-3B, 1A-4H, and 3B-4H; Supplementary Table S3). Correct targeting of the *Zfy1* in *Zfy2* KO ESC clones was determined by PCR analysis using primers shown in Supplementary Table S2. All six clones had the *Zfy1* deletion removing *Zfy1* ORF in the context of the same *Zfy2* deletion as in the parental *Zfy2* null ESC, were confirmed to be chromosomally normal (73–91% cells having 40 chromosomes), and were used to make chimeric F0 founders.

Production of *Zfy2* KO and *Zfy* DKO mice

Targeted ESCs were injected into 8-cell stage or blastocyst-stage host CD-1 embryos. The manipulated embryos were transferred to pseudopregnant recipients. Chimeric mice (F0) were identified at birth by presence of black eyes and GFP fluorescence, and a week later by a coat color. Chimeric males were mated to C57BL/6 females to test for germline transmission. In cases when the chimeric males failed to induce pregnancy, assisted reproduction (ICSI if sperm were found and ROSI when only spermatids were available) was done to produce the next generation offspring. Successful germline transmission was identified by PCR genotyping using primers shown in Supplementary Table S2. The loss of *Zfy2* (*Zfy2* KO) or *Zfy1* and *Zfy2* (*Zfy* DKO) was confirmed in F1 progeny by sequencing and transcript expression analysis. The phenotype characterization was performed with F1 males that were at least 67.5% C57BL/6 genetic background. *Zfy2* KO and *Zfy* DKO F1 males were subsequently backcrossed to C57BL/6 genetic background by mating and assisted reproduction, respectively.

Genotyping

The presence of *Zfy1* and *Zfy2* mutations were confirmed by PCR genotyping in targeted ESC and in mice, using primers shown in Supplementary Table S2. All mice were tested for both an intact and a mutated versions of *Zfy*, so that the presence or absence of the amplicon was confirmed in two independent assays. Positive, negative, and blank controls were included in every assay.

Off-target analysis

Two putative off-target sites per gRNA were predicted by NCBI Blast online software (https://blast.ncbi.nlm.nih.gov/Blast.cgi) (Supplementary Table S4). The off-target sites were PCR-amplified (primer sequences are shown in Supplementary Table S2) and directly sequenced.

RNA isolation and RT-PCR

RNA was isolated from testes using RNAeasy Micro Kit (Qiagen, 74004, Valencia, CA, USA) following manufacturer's instructions. Reverse transcription of polyadenylated RNA was performed with Superscript IV Reverse Transcriptase, according to the manufacturer's guidelines (Invitrogen, 18090050, Carlsbad, CA, USA). *Zfy* transcript expression was measured qualitatively in cDNA by PCR followed by gel electrophoresis. At least three biological samples were used for each genotype. Primers sequences are shown in Supplementary Table S2.

Fecundity testing

The fertility of *Zfy*-deficient males and wild-type (WT) controls was assessed over a period of 6 weeks by mating with mature CD-1 females (either 1 or 2 females per male). For males for which pregnancy was not observed, the occurrence of mating was confirmed by checking for presence of copulatory plugs.

Assisted reproduction

Oocyte collection

Female mice were induced to superovulate with the injection of 5 IU eCG and 5 IU hCG given 48 h apart. Oocyte collection and subsequent oocyte manipulation, including in vitro fertilization and microinjections, were done in HEPES-CZB [25]), with subsequent culture in CZB medium [26] in an atmosphere of 5% CO_2 in air.

In vitro fertilization (IVF)

IVF was as described by us before [27]. For IVF, the epididymal sperm were expressed from dissected caudae epididymides directly into a drop of HTF medium [28] (capacitation drop) and sperm concentration was quantified. Sperm were capacitated in HTF for 1.5 h at 37°C in a humidified atmosphere of 5% CO2. Then, a portion of capacitated sperm suspension was transferred to another drop of HTF medium (fertilization drop) to achieve a concentration of 5×10^6/mL. For zona-intact IVF, oocyte-cumulus cell complexes were released to the fertilization drop and gametes were co-incubated for 4 h. For zona-free IVF, oocyte-cumulus cells complexes were dispersed with hyaluronidase (1 mg/mL in HEPES-CZB), zona pellucidas were removed with acidic Tyrode's solution (pH 2.5) [29], zona-free oocytes were then introduced to fertilization drop, and gametes were co-incubated for 4 h. After co-incubation, the oocytes were washed several times with HEPES-CZB, followed by at least one wash with CZB. Embryos were cultured in CZB and observed at different time points for proper development: 6 h (PN stage), 24 h (2-cell stage), 48 h (4- or 8-cell stage), 72 h (morula or early blastocyst), and 96 h (blastocyst/expanded blastocyst). The oocytes after zona-free IVF were not scored for development beyond PN stage.

Intracytoplasmic sperm injection

ICSI was carried out as described by us before [30], within 1–2 h from oocyte and sperm collection. Sperm-injected oocytes were transferred in CZB and cultured at 37°C. The survival and activation of injected oocytes was scored 1–2 and 6 h after the commencement of culture, respectively. The oocytes with two well-developed pronuclei and extruded second polar body were considered activated.

Round spermatid injection

ROSI was carried out as described by us before [31]. Briefly, to obtain round spermatids, testes were dissected, and testicular cell suspension was diluted with HEPES-CZB containing 1% (w/v) polyvinyl pyrrolidone (PVP) (MP Biomedicals, 102787) on the injection dish. Round spermatids were injected individually into the oocytes. The total duration of ROSI was no longer than 1 h. The oocytes were activated shortly after injection by incubation in Ca^{2+}-free CZB medium supplemented with 2.5 mM strontium chloride ($SrCl_2$, Sigma, 31,362) at 37°C, 5% CO_2 for 4 h, after which time they were transferred

into standard CZB medium for subsequent culture. At ~6–8 h after injection, the oocytes were assessed for polar body extrusion and pronuclei development, and 24 h after injection for cleavage.

Embryo transfer

Embryo transfer was performed with the 2-cell embryos derived from normally fertilized oocytes resulting from ICSI or ROSI. Surrogate mothers were allowed to deliver on their own or were subjected to cesarian section on day 20 of pregnancy followed by fostering of pups.

Basic sperm analyses

To analyze sperm number, motility, and morphology, cauda epididymal sperm were released into HEPES-CZB medium and incubated for at least 10 min at 37°C immediately before analysis. Sperm counts done using a hemocytometer were the mean of three independent scorings per sample. Motility assessment was done by manual scoring with at least 100 sperm scored per male. For motility, a proportion of all motile sperm (both progressively motile and nonprogressively motile) was defined. For the analysis of sperm morphology, epididymal sperm were stained with silver nitrate as previously described [32]. Briefly, the sperm suspension (diluted as necessary with 0.9% NaCl) was smeared on three slides, allowed to dry, fixed in methanol and acetic acid (3:1), and stained with silver nitrate. The slides were coded and 100 sperm heads per slide were viewed at 1000× magnification and scored in a blind fashion.

Testis histology analysis

For histology analysis, portions of the testes were fixed in Bouin overnight and then stored in 70% ethanol prior to embedding in paraffin wax, sectioning at 5 μm, and staining with hematoxylin-eosin (H&E) and Periodic acid-Schiff and hematoxylin (PAS-H). The stages of seminiferous tubules were identified based on the composition of cells near the basal membrane according to the method described by Ahmed and de Rooij [33]. This was necessary because of meiotic and post-meiotic arrests present in males lacking both *Zfy1* and *Zfy2*, which prevented staging based on the changes of acrosome and nuclear morphology of spermatids. Quantitative analysis of spermatogenesis progression and seminiferous epithelium abnormalities were done as described by us before [34]. For each male, 10 tubules were examined per stage category and the numbers of spermatogonia, round spermatids, and Sertoli cells were counted. The data were expressed as germ cell/Sertoli cell ratios. The analysis of seminiferous epithelium abnormalities was done concurrently with quantitative analysis of spermatogenesis progression, such that any abnormal cells matching the categories described below were quantified, while germ cell and Sertoli cell counts were being done.

Transmission electron microscopy

Epididymal sperm and testis tissue were fixed in 2.5% glutaraldehyde, 0.1 M sodium cacodylate, 2 mM calcium chloride, pH 7.4, 1 h, then postfixed with osmium tetroxide (1% in 0.1 M cacodylate buffer, 1 h), dehydrated in ethanol, substituted with propylene oxide, and embedded in LX-112 epoxy resin. Ultra-thin sections (60–80 nm) were collected on Formvar-coated copper grids, double stained with uranyl acetate and lead citrate, and viewed a Hitachi HT7700 transmission electron microscopy (TEM) at 100 kV, and photographed with an AMT XR-41B 2 k x 2 k CCD camera at ×3000–4000 original magnification.

Experimental design and statistics

Student *t*-test was used for most analyses, with $P < 0.05$ considered as statistically significant difference. If data were expressed as percentages, the percentages were converted to angles for statistical analyses. One- or two-way ANOVA with a post-hoc test was also used in some analyzes. A nonparametric Pearson Chi-square test for independence with a Monte Carlo simulation was used as an additional test for TEM analyses. Computations were done using Excel for GraphPad Prism.

Results

Generation of *Zfy1* KO, *Zfy2* KO, and *Zfy* DKO mice

Zfy1 KO males were produced by direct zygote targeting. Founder F0 males obtained after embryo transfer were screened for successful targeting using PCR and sequencing. Three F0 males (#14, #16, and #20) were shown to carry the *Zfy1* KO allele and provided sperm for ICSI with B6 oocytes to produce F1 *Zfy1* KO males. The obtained F1 male offspring were tested for presence of the deletion by PCR analysis and sequencing, and all were shown to have a complete loss of *Zfy1* (Figure 1 and Supplementary Figure S1). The F1 males were then used for phenotype characterization.

Zfy2 KO and DKO mice were generated by creating chimeric mice via embryonic stem cells (ESC) injection. To distinguish the mutant ESC-derived cells from the WT host cells, ESC clones were established from double transgenic mice expressing EGFP ubiquitously (Supplementary Figure S2A) and in the sperm acrosome [21]. Thus, observation of green fluorescence in chimeric embryos (Supplementary Figure S2B) and in body of newborn pups was indicative of chimerism, and in isolated spermatogenic cells (round/elongating spermatids and sperm) of a mutation present in germline (Supplementary Figure S2C). It also allowed to use EGFP expression to select spermatids and sperm carrying the mutation for assisted reproduction (Supplementary Figure S2C).

For *Zfy2* KO, three ESC clones (1C, 3B, and 4H) were shown to be successfully targeted with a deletion removing the entire *Zfy2* ORF by PCR analysis followed by sequencing and were used to make chimeric F0 founders. A total of 10 F0 chimeric males were obtained, all but one were fertile, and two fertile males (1C.1 and 4H.1) transmitted the targeted allele to the next generation, yielding *Zfy2* KO F1 males (Supplementary Table S3). The KO was confirmed by PCR genotyping, sequencing, and testing for presence of *Zfy2* transcripts (Figure 1 and Supplementary Figure S3). The F1 males were used for phenotype characterization and to backcross the line to C57BL/6 genetic background.

For *Zfy* DKO, 6 ESC clones were shown to have a deletion of *Zfy1* ORF and *Zfy2* ORF and were used to make chimeric F0 founders. A total of 16 F0 chimeric males were obtained (Supplementary Table S3). Twelve F0 males were fertile and 4 were infertile. All males were checked for presence of EGFP positive germ cells and 11 were shown to have green sperm or green round spermatids. Four *Zfy* DKO F0 males

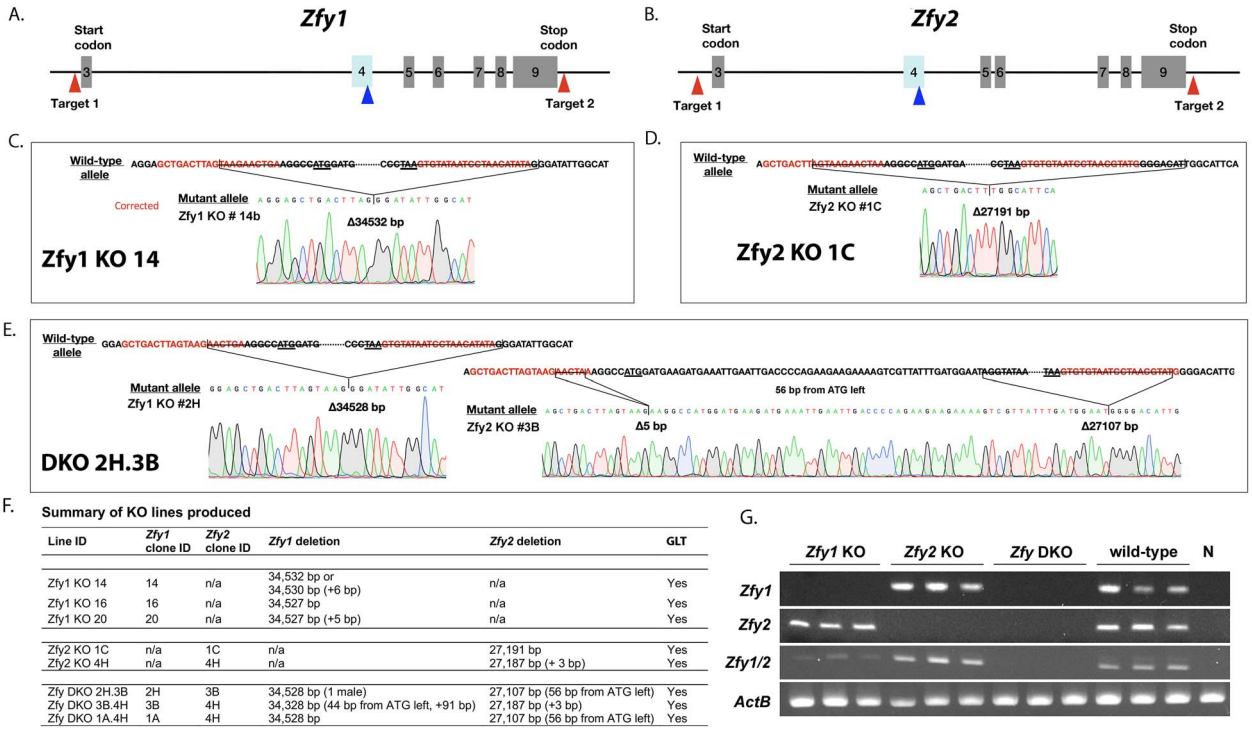

Line ID	Zfy1 clone ID	Zfy2 clone ID	Zfy1 deletion	Zfy2 deletion	GLT
Zfy1 KO 14	14	n/a	34,532 bp or 34,530 bp (+6 bp)	n/a	Yes
Zfy1 KO 16	16	n/a	34,527 bp	n/a	Yes
Zfy1 KO 20	20	n/a	34,527 bp (+5 bp)	n/a	Yes
Zfy2 KO 1C	n/a	1C	n/a	27,191 bp	Yes
Zfy2 KO 4H	n/a	4H	n/a	27,187 bp (+ 3 bp)	Yes
Zfy DKO 2H.3B	2H	3B	34,528 bp (1 male)	27,107 bp (56 bp from ATG left)	Yes
Zfy DKO 3B.4H	3B	4H	34,328 bp (44 bp from ATG left, +91 bp)	27,187 bp (+3 bp)	Yes
Zfy DKO 1A.4H	1A	4H	34,528 bp	27,107 bp (56 bp from ATG left)	Yes

Figure 1. Generating of *Zfy* KO mice. (A and B) *Zfy1* and *Zfy2* gene exon structure with the sgRNA target loci. Red triangles show the target loci in this study, a blue triangle show the target locus in the study of Nakasuji et al. [17]. Alternatively spliced exon 4 which is shown in pale blue color. (C–E) Exemplary mutation of *Zfy1* KO (C), *Zfy2* KO (D), and *Zfy* DKO (E) F1 mice. In WT alleles, red font indicates target sequence, start and stop codons are underlined, deleted sequence is crossed, and mutant alleles are shown as raw sequencing waveform data with the insertion/deletion lengths indicated. (F) Summary of produced KO lines. All produced mutant alleles are shown as raw sequencing waveform in Supplementary Figures S1, S3, and S4). GLT, germline transmission. (G) *Zfy* transcript expression. Expression of transcripts specific to *Zfy1*, *Zfy2*, and both *Zfy1* and *Zfy2* (*Zfy1/2*) was measured in whole testes lysates from *Zfy1* KO, *Zfy2* KO, and *Zfy* DKO males, with WT males serving as a positive control and XO*Sry* (N) male, which lacks Y chromosome, as a negative control. Expression was assayed by RT-PCR, with *ActB* serving as an amplification control. *Zfy1* KO and *Zfy2* KO males lacked expression of *Zfy1* and *Zfy2*, respectively, and retained the homologous and combined transcripts. *Zfy* DKO males lacked all measured transcripts.

(2H.3B.1, 2H.3B.2, 3B.4H.2, and 1A.4H.4) yielded F1 male offspring after ICSI with green sperm or after ROSI with green spermatids (Supplementary Table S3). Presence of double knockout in F1 males was confirmed by PCR genotyping, sequencing, and testing for presence of *Zfy* transcripts (Figure 1 and Supplementary Figure S4). The *Zfy* DKO F1 males were used for phenotype characterization, and to backcross the line to C57BL/6 genetic background.

To address the possibility of potential off-target effects of CRISPR/Cas9, two putative off-target sites for each of the four gRNAs were computationally predicted, amplified by PCR, and directly sequenced, with three randomly selected males tested per knockout line. None of the males has shown any mutation in any of the sites tested (Supplementary Figure S5).

Fertility assessment of *Zfy1* KO, *Zfy2* KO, and *Zfy* DKO males

Zfy1 KO, *Zfy2* KO, and *Zfy* DKO F1 males were subjected to fecundity testing. We quantified time from the beginning of mating to delivery of the 1st litter, litter size, and sex ratio (Table 1). The WT controls for *Zfy2* KO and *Zfy* DKO males were mutation-free offspring obtained from F0 chimeric males without GLT (WT sibs). For *Zfy1* KO, controls were WT C57BL/6 males from our colony (WT). Sixteen *Zfy1* KO males were tested, and all were fertile. No differences between *Zfy1* KO and controls were observed for any of the parameters (Table 1). For *Zfy2* KO, 16 out of 18 males tested (89%) were fertile. The time since commencement of mating to the 1st litter delivery and the sex ratio were like those observed with controls, but the average litter size was lower (7–9 for *Zfy2* KO males vs. 13 for controls, Table 1). When *Zfy1* KO and *Zfy2* KO males were compared with each other, *Zfy1* KO males had larger litters (13 ± 0.6 vs. 8 ± 0.7, $P < 0.0001$).

For *Zfy* DKO, all 16 tested males were confirmed to plug females, but none induced pregnancy. Sperm from *Zfy* DKO males also failed to fertilize oocytes in vitro, even with sperm number adjusted to be compatible with IVF), and with zona-free oocytes (Figure 2). During IVF trials, we observed increased incidence of sperm tail bending and folding, which might have affected sperm fertilization ability (Supplementary Figure S6). For 12 of *Zfy* DKO males, haploid gametes (sperm or spermatids) were injected into the oocytes, and all males yielded offspring (Supplementary Table S5).

Together, the data show that single *Zfy* KO does not impede male fertility but loss of both *Zfy* homologues renders males completely infertile. The data also suggest that *Zfy2* KO males have mildly impaired breeding efficiency. Finally, the data show that infertility of *Zfy* DKO males is due to sperm inability to successfully fertilize oocytes on their own and not due to the deficiency in what sperm contribute to the oocyte after fertilization.

Table 1. Fertility assessment of *Zfy* KO males

Line	Fertile males/males tested	Cohabitation days to 1st litter (days) (mean ± SEM)	No of litters examined	Litter size (mean ± SEM)	No of pups obtained (female/male)
Zfy1 KO 20	8/8	23 ± 0.91	16	14 ± 0.92	205 (95/110)
Zfy1 KO 14	8/8	24 ± 1.49	18	12 ± 0.75	186 (94/94)
WT[#]	4/4	27 ± 2.4	10	12 ± 0.44	118 (66/54)
Zfy2 KO 1C	8/10	28 ± 1.98	18	9 ± 1.03[a]	166 (88/78)
Zfy2 KO 4H	8/8	26 ± 1.84	22	7 ± 0.82[c]	159 (78/81)
WT sibs	4/4	28 ± 0.71	12	13 ± 0.89	155 (75/80)
Zfy DKO 3B.4H	0/7	n/a	n/a	n/a	n/a
Zfy DKO 1A.4H	0/2	n/a	n/a	n/a	n/a
Zfy DKO 2H.3B	0/7	n/a	n/a	n/a	n/a
WT sibs	5/5	21.4 ± 0.48	10	13 ± 0.50	169 (98/71)

All males were bred for 6 weeks starting at 8 weeks of age. [#]All F1 males obtained after ICSI had mutation, so negative siblings were not available and WT males on the same genetic background and of the same age were used as controls. Statistical significance (*t*-test): KO/DKO mice were compared with their specific WT controls. [a]<0.05; [c]<0.001.

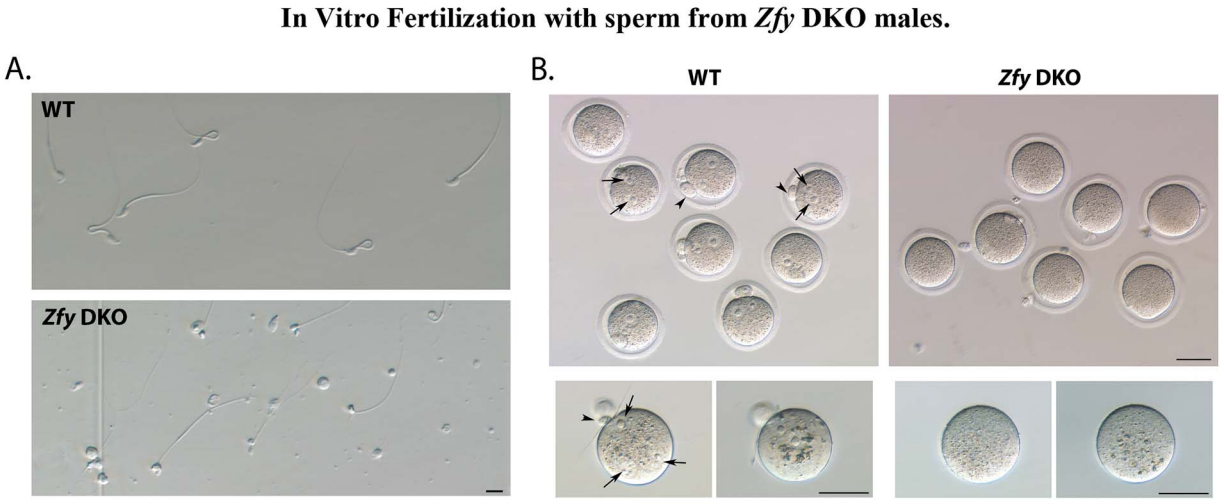

C.

Exp.	Male	Oocyte donor (strain)	Oocyte status	No oocytes inseminated	No of oocytes activated (monospermic/ multispermic)[#]	No of 2-cell embryos (%)[a]	No of 4-8-cell embryos (%)[b]	No of M/EB (%)[b]	No of B/ExB (%)[b]
1	*Zfy* DKO	CD-1	ZP intact	17	0	0	0	0	0
	Zfy DKO	CD-1	ZP-free	11	0	n/a	n/a	n/a	n/a
	WT	CD-1	ZP-intact	41	31 (31/0)	29 (71)	28 (90)	28 (90)	26 (83)
2	*Zfy* DKO	CD-1	ZP intact	19	0	0	0	0	0
	Zfy DKO	CD-1	ZP-free	10	0	n/a	n/a	n/a	n/a
	Zfy DKO	C57BL/6	ZP-free	19	0	n/a	n/a	n/a	n/a
	WT	CD-1	ZP-intact	19	8 (8/0)	8 (42)	8 (100)	8 (100)	8 (100)
	WT	C57BL/6	ZP-free	22	22 (12/10)	n/a	n/a	n/a	n/a
3	*Zfy* DKO	CD-1	ZP intact	20	0	0	0	0	0
	Zfy DKO	CD-1	ZP-free	19	0	0	0	0	0
	WT	CD-1	ZP-intact	17	10 (10/0)	10 (59)	10 (100)	10 (100)	10 (100)
	WT	CD-1	ZP-free	18	18 (12/6)	n/a	n/a	n/a	n/a

M, morula; EB, early blastocyst; B, blastocyst; ExB; expanded blastocyst. Percentage was calculated: [a] from oocytes inseminated; [b] from 2-cell embryos. Sperm concentration during IVF was always the same (5 x 10^6/mL) for all groups and for all replicates. [#] Monospermic activation results in 2 pronuclei and extruded 2nd polar body; Multispermic activation results in 3 or more pronuclei and extruded 2nd polar body.

Figure 2. Sperm function in in vitro fertilization. In vitro fertilization was performed with sperm from *Zfy* DKO (A, bottom) and from WT males serving as a control (A, top) and either zona pellucida (ZP)-intact (B, top) or ZP-free (B, bottom) oocytes. Six hours after the end of gamete co-incubation signs of fertilization expressed as development of pronuclei (examples shown with arrows), and extrusion of the 2nd polar body (examples shown with arrowheads) could be seen after oocyte insemination with sperm from WT but not sperm from developing embryos were obtained after IVF with sperm from WT males. No embryos were obtained after IVF with sperm *Zfy* DKO males (C). Scale is 10 μm in A and 50 μm in B.

Table 2. Sperm quality assessment of *Zfy* KO males

Line (no males)	Age at analysis (wks)	Average ± SDev			
		Body weight (g)	Testis weight (mg)	Sperm number ($\times 10^6$, 1 epi)	Motile sperm (%)
Zfy1 KO 14 ($n = 5$)	17	35 ± 1.7[a]	109 ± 3.7	20 ± 7.6[a]	43 ± 7.1
Zfy1 KO 16 ($n = 3$)	17	40 ± 1.3[b]	112 ± 7.2	16 ± 9.2	52 ± 17.9
Zfy1 KO 20 ($n = 7$)	17	35 ± 2.4[a]	110 ± 5.6	13 ± 3.2[a]	33 ± 9.6
WT[#] ($n = 4$)	18	30 ± 3.9	109 ± 3.9	7 ± 2.49	34 ± 10.9
Zfy2 KO 1C ($n = 8$)	12-15	32 ± 4.1	106 ± 13.9[b]	6 ± 2.8	28 ± 17.7
Zfy2 KO 4H ($n = 8$)	16	33 ± 4.6	108 ± 11.8[b]	12 ± 3.0	40 ± 7.5[a]
WT sibs ($n = 4$)	16	33 ± 5.0	119 ± 7.03	9 ± 3.3	25 ± 10.9
Zfy DKO 3B.4H ($n = 7$)	16	46 ± 6.7	86 ± 12.5[c]	1.24 ± 1.1[c]	16 ± 12.3
Zfy DKO 1A.4H ($n = 1$)	17	37 ± 0.0	85 ± 1.4[c]	0.04 ± 0.0[a]	15 ± 0.0
Zfy DKO 2H.3B ($n = 6$)	17-18	39 ± 5.7	77 ± 12.9[c]	1.02 ± 0.7[c]	19 ± 12.1
WT sibs ($n = 5$)	17	41 ± 6.3	149 ± 6.3	16.12 ± 4.3	17 ± 6.3

All examined males were F1 generation. [#]All F1 males obtained after ICSI had mutation, so negative siblings were not available and WT males on the same genetic background and of the same age were used as controls. Statistical significance (*t*-test): KO/DKO mice were compared with their specific WT controls. [a]<0.05; [b]<0.01; [c]<0.001.

Spermiogenic phenotype of *Zfy1* KO, *Zfy2* KO, and *Zfy* DKO males

We next characterized basic sperm parameters for *Zfy1* KO, *Zfy2* KO, and *Zfy* DKO F1 males (Table 2). *Zfy1* KO males had normal body weight, testis weight, and sperm number and motility. Similar observations were made for *Zfy2* KO males, with some decrease in testis size when compared with controls, but overall, with all measured parameters remaining within a normal range. Interestingly, sperm from one of *Zfy2* KO lines (line 4H) displayed higher sperm motility than that of controls. The difference in motility in two groups of WT sibs was likely a batch effect as these mice were derived and examined ~1.5 year apart. When *Zfy1* KO and *Zfy2* KO males were compared with each other, *Zfy2* KO produced fewer sperm ($16 \times 10^6 \pm 0.25$ vs. $9 \times 10^6 \pm 1.06$, $P < 0.0012$). The caveat of this comparison is that *Zfy1* KO F1 males were on pure C57BL/6 genetic background while *Zfy2* KO F1 were 75% C57BL/6. However, as *Zfy2* KO males were backcrossed to C57BL/6, their sperm number remained under 10×10^6/epididymis, with the fully backcrossed males (10 generations backcross) averaging 5.9×10^6/epididymis.

The *Zfy* DKO males had body weight similar to controls, but their testis size was significantly decreased, and sperm number was drastically decreased when compared with controls ($<1.5 \times 10^6$ vs. 16×10^6). The motility of the few sperm that were produced was normal. Similar phenotype was observed in F2 generation of *Zfy* DKO males (produced by ART) (Supplementary Table S6). Interestingly, high number of sloughed round cells could be seen in epididymis from *Zfy* DKO males (Supplementary Figure S7).

Since sperm morphology defects are common in mice with Y chromosome deficiencies, including mice lacking *Zfy* genes [15, 32, 35], we performed analysis of epididymal sperm headshape on silver-stained testicular cell spreads for both *Zfy* KO and DKO males (Figure 3). We divided the observable headshape types into normal (N) and eight defect categories (1–8) (Figure 3A) and quantified their incidence (Figure 3B). In WT control males, almost all sperm had normal headshape, and few that did not, had the mildest headshape defect type (score 1). *Zfy1* KO males had most sperm classified as score 1, with the remainder either normal or presenting with other mild headshape defects (score 2 and 3). *Zfy2* KO males had no morphologically normal sperm, and all types of headshape defects were observed, with scores 3 (33% of sperm) and 5 (21% of sperm) being the most common, and the severe headshape defects (scores 6–8) affecting 21% of sperm. *Zfy* DKO males also had no sperm with normal headshapes, and the defects were much more severe, with more than 70% of sperm having score 7 or 8.

Together, the data support that loss of *Zfy2* negatively affects sperm number and morphogenesis, and specifically sperm head elongation and curvature, and this is further exacerbated when both *Zfy1* and *Zfy2* are lost. However, presence of *Zfy1* is not required for normal sperm production and normal sperm headshape.

Spermatogenesis progression and normalcy is impaired in *Zfy* DKO males

Since *Zfy* DKO males had the most severe spermiogenic phenotype coupled with infertility, we characterized these males more comprehensively and performed quantitative histological assessment of spermatogenesis on testis sections, in a similar manner as we did in our past studies [31, 34]. F1 DKO males, with distinction between males produced by ICSI and by ROSI, were included in analyses (Table 3, Figure 4B). The numbers of spermatogonia and Sertoli cells in *Zfy* DKO males were similar as in controls. The number of postmeiotic cells, however, was significantly depleted. Both ICSI- and ROSI-derived *Zfy* DKO males had about 2-fold fewer round spermatids than controls. The number of elongating/elongated spermatids was more depleted, 4-fold fewer and 9-fold fewer for ICSI- and ROSI-derived *Zfy* DKO males, respectively.

Classic murine spermatogenesis staging relies on Periodic acid-Schiff staining (PAS) to identify the morphology of the acrosome. PAS staining can also be used to evaluate germ cell degeneration [36]. Spermatogenesis staging and germ cell counts were performed concurrently with the abnormality identification. Nuclear morphology, nucleosomal patterning, cell size, cell location, and cytoplasmic appearance were used to identify cellular abnormalities in the seminiferous tubules in a similar manner as we described before for males with limited Y chromosome gene contribution [34]. We differentiated and quantified the following cellular defects: apoptotic cell (AC), apoptotic cell at meiotic metaphase (AM), degenerating

Table 3. Quantitative analysis of spermatogenesis progression

Genotype	Spermatogonia/Sertoli cell ratio (mean ± SEM)						
	XII-I	**II-IV**	**V-VI**	**VII-VIII**	**IX-X**	**XI**	**All stages**
XY ($n = 3$)	1.22 ± 0.25	1.94 ± 0.14	2.97 ± 0.06	0.63 ± 0.07	0.63 ± 0.02	1.01 ± 0.10	1.40 ± 0.05
XY *Zfy* DKO ICSI ($n = 4$)	1.05 ± 0.02	1.85 ± 0.15	2.95 ± 0.21	0.53 ± 0.05	0.60 ± 0.06	0.73 ± 0.04*	1.27 ± 0.07
XY *Zfy* DKO ROSI ($n = 6$)	1.03 ± 0.16	1.82 ± 0.18	2.96 ± 0.21	0.50 ± 0.03	0.66 ± 0.06	0.79 ± 0.06	1.25 ± 0.06
XY *Zfy* DKO All ($n = 10$)	1.04 ± 0.09	1.83 ± 0.12	2.95 ± 0.14	0.51 ± 0.03	0.63 ± 0.04	0.77 ± 0.04*	1.26 ± 0.04
	Round spermatid/Sertoli cell ratio (mean ± SEM)						
	XII-I	II-IV	V-VI	VII-VIII	IX-X	XI	All stages
XY ($n = 3$)	10.51 ± 2.75	19.35 ± 0.95&	18.91 ± 1.47&	16.57 ± 1.53&	0.00 ± 0.00	0.00 ± 0.00	11.03 ± 1.15&
XY *Zfy* DKO ICSI ($n = 4$)	6.46 ± 0.89	10.04 ± 1.17	10.33 ± 1.57	9.38 ± 2.02	0.15 ± 0.09	0.03 ± 0.03	5.98 ± 0.92
XY *Zfy* DKO ROSI ($n = 6$)	5.20 ± 1.14	7.09 ± 0.83	7.92 ± 1.02	4.98 ± 1.30	0.02 ± 0.02	0.00 ± 0.00	4.01 ± 0.56
XY *Zfy* DKO All ($n = 10$)	5.70 ± 0.76*	8.27 ± 0.80	8.89 ± 0.91	6.74 ± 1.28	0.07 ± 0.04	0.01 ± 0.01	4.80 ± 0.56
	Elongating and elongated spermatid/Sertoli cell ratio (mean ± SEM)						
	XII-I	II-IV	V-VI	VII-VIII	IX-X	XI	All stages
XY ($n = 3$)	21.46 ± 1.31&	22.37 ± 1.44&	21.31 ± 2.28&	16.61 ± 1.48&	19.58 ± 1.08&	24.43 ± 1.74&	20.82 ± 1.29&
XY *Zfy* DKO ICSI ($n = 4$)	6.53 ± 2.14	5.29 ± 2.07	3.99 ± 1.55	4.36 ± 2.08	6.61 ± 2.48	6.93 ± 2.47	5.61 ± 2.09
XY *Zfy* DKO ROSI ($n = 6$)	2.98 ± 0.45	2.11 ± 0.44	1.90 ± 0.44	1.67 ± 0.36	3.18 ± 0.57	3.53 ± 1.11	2.52 ± 0.45
XY *Zfy* DKO All ($n = 10$)	4.40 ± 1.01	3.38 ± 0.95	2.74 ± 0.71	2.74 ± 0.90	4.55 ± 1.11	4.89 ± 1.24	3.76 ± 0.95
	Sertoli cell number (mean ± SEM)						
	XII-I	II-IV	V-VI	VII-VIII	IX-X	XI	All stages
XY ($n = 3$)	60.67 ± 6.64	57.33 ± 2.91	64.00 ± 4.51	62.00 ± 4.51	63.67 ± 4.70	53.67 ± 4.81	361.33 ± 26.39
XY *Zfy* DKO ICSI ($n = 4$)	68.00 ± 3.92	69.25 ± 3.97	65.50 ± 3.12	66.75 ± 4.87	69.25 ± 6.42	73.00 ± 6.36	411.75 ± 22.54
XY *Zfy* DKO ROSI ($n = 6$)	65.33 ± 7.82	67.17 ± 3.93	61.67 ± 6.60	63.50 ± 4.50	64.83 ± 4.82	73.50 ± 7.42	396.00 ± 28.55
XY *Zfy* DKO All ($n = 10$)	66.40 ± 4.75	68.00 ± 2.71	62.30 ± 4.03	64.80 ± 3.19	66.60 ± 3.71	73.30 ± 4.88	402.30 ± 18.60

XY *Zfy* DKO ICSI and *Zfy* DKO ROSI are *Zfy* DKO F1 males produced by ICSI and ROSI, respectively. XY are mutation-free siblings obtained from F0 males. For each male, 10 tubules were examined per stage, and the numbers of Sertoli cells, spermatogonia, round spermatids, and elongating and elongated spermatids were counted. The data are expressed as germ cell/Sertoli cell ratios. In WT males, no round spermatids are present in stages IX–XI, so those observed in the remaining genotypes represent "delayed spermatids." Statistical significance (*t*-test, $P < 0.05$). *Different than XY. &Different from all other.

nucleus (DN), hypercondensed nucleus (HN), multinucleated giant cell (MGC), cell remnant (CR), sloughed Sertoli cell (SS), and vacuole (V) [34] (Figure 4).

Some abnormalities of seminiferous epithelium were observed in control males, but *Zfy* DKO males had ~3-fold (ICSI) and ~6-fold (ROSI) more defects (Figure 4A and B). When the incidences of specific defect types were quantified, AC and HN defects were the most abundant in both the control and the *Zfy* DKO males. *Zfy* DKO males presented with significantly more AC, DN, and MGC than controls, while HN was more frequently seen in control testis (Figure 4C).

Overall, the data confirm that spermatogenesis progression is severely abnormal in *Zfy* DKO males, with decreased development of postmeiotic cells, impaired spermiogenesis, and increased incidence of seminiferous epithelium defects.

Sperm from *Zfy* DKO males have structural defects within head and tail, with acrosome alterations appearing early during spermiogenesis

Considering that *Zfy* DKO males had the most severe sperm headshape defects, we used TEM to further evaluate normalcy of head and tail of epididymal sperm from *Zfy* DKO males, with WT males serving as control. Five *Zfy* DKO males and 2 WT males were included in this analysis, with 30 sperm examined per male.

Sperm head analysis included assessments of membrane integrity, acrosome normalcy, and chromatin condensation (Figure 5A and B). With respect to membrane integrity, we assigned examined sperm heads into three categories reflective progressive membrane changes: intact membrane (IM), broken membrane (BM, and disintegrating membrane (DM). When examining chromatin condensation, we categorized sperm into those with condensed chromatin (CC), slightly decondensed chromatin (SLDC), and severely decondensed chromatin (SVDC) chromatin. With assessment of acrosome, we categorized sperm into those with intact acrosome (IA), irregular acrosome (IRA) and separate acrosome (SA), separate. Data analysis using two-way ANOVA revealed no effect of genotype (*Zfy* DKO vs. control) for any of the examined structures (membrane, acrosome, chromatin). However, paired comparisons done with the post-hoc test have shown that *Zfy* DKO males had significantly more sperm with membrane and acrosome defects (Figure 5B).

Tail analysis included assessment of normalcy of mitochondria, axoneme, and outer dense fibers (Figure 5C and D). With respect to mitochondria, we classified sperm tails as normal "NMi", abnormal "AMi", and severely abnormal "SAMi". Axoneme and Outer Dense Fiber organization was classified as organized (OA and OF) or disorganized (DA and DF). When the data were analyzed with two-way ANOVA, no effect of genotype was observed. Similarly as it was with sperm head assessment, paired comparisons done with the post-hoc test have shown that *Zfy* DKO males had significantly more sperm with mitochondria and axoneme defects (Figure 5D).

Because the number of sperm examined by TEM was low, caused by very low epididymal sperm number in these males (Table 2), we performed an additional data analysis: a non-parametric Pearson Chi-square test for independence with a Monte Carlo simulation to simulate a sample size of 2000, which gives more power to the statistical analysis and allows to assess whether significance would be present in a much larger sample set. With this analysis, all p-values were significant (Supplementary Figure S8).

We next asked whether the structural and morphological defects observed in epididymal sperm arose during spermiogenesis, a process during which haploid round spermatids undergo a variety of changes to become mature sperm. To test this, we performed TEM analysis of testis samples, focusing on two features of round spermatids: curvature, differentiating between smooth curve (SC) and non-smooth curve (NSC), and normalcy of the acrosome in its early stage of development, classifying it as either intact (IA) or irregular (IRA) (Supplementary Figure S9). Five *Zfy* DKO males and 1 control male were used for this analysis with approximately 30 photos were taken for each male. The spermatids were photographed between the Golgi and the acrosome phase [37]. No differences between *Zfy* DKO and controls were found with two-way ANOVA analysis (Supplementary Figure S9B), while the Pearson Chi-square test with a Monte Carlo simulation revealed significant difference in assessment of the developing acrosome, but not cell curvature (Supplementary Figure S9C).

Overall, the data support that the loss of both *Zfy1* and *Zfy2* leads to the fragility of sperm membrane and structural defects of sperm head and tail, including defects of acrosome, mitochondria, and axoneme, and that the acrosome defects begin to appear early during spermiogenesis.

Loss of *Zfy1* leads to overexpression of *Zfy2*

Considering the differences in phenotype of *Zfy1* KO and *Zfy1*, we quantified transcript level of *Zfy1*, *Zfy2*, and global *Zfy* (*Zfy1/2*) in whole testes from all three KO models. As expected, *Zfy1* KO males lacked *Zfy1* expression, *Zfy2* KO males lacked *Zfy2* expression, and *Zfy* DKO males lacked both *Zfy1* and *Zfy2* expression. Interestingly, loss of *Zfy1* led to overexpression of *Zfy2*; even though the difference did not reach statistical significance, *Zfy2* transcripts level in *Zfy1* KO was clearly elevated when compared with expression in control WT males (Supplementary Figure S10). This translated to global levels of *Zfy1/2* transcripts in *Zfy1* KO higher than in *Zfy2* KO, and comparable to those of WT males.

Discussion

This study is an extension of our previous work focusing on characterization of the function of Y chromosome genes *Zfy1* and *Zfy2*. Using mice with Y chromosome deficiencies and supplementing *Zfy* transgenes, we have shown before that the loss of *Zfy1* and *Zfy2* is associated with infertility and various spermiogenic defects, and that the addition of transgenes allows to rescue these deficiencies [13, 15]. Using the same mouse models, similar observations were made by other investigators [10–12, 14, 38]. Because of limitations imposed by these experimental models, where the loss of *Zfy* was linked to the loss of other Y genes, we generated mice with CRISPR/Cas9-mediated complete KO of *Zfy* genes and characterized their phenotype.

Consequences of a single *Zfy* gene knockout

We demonstrated that loss of either *Zfy1*, or *Zfy2*, individually, did not lead to male infertility. However, when two single KOs were compared, males lacking *Zfy2* had smaller litters, fewer sperm, and increased incidence of sperm with headshape defects.

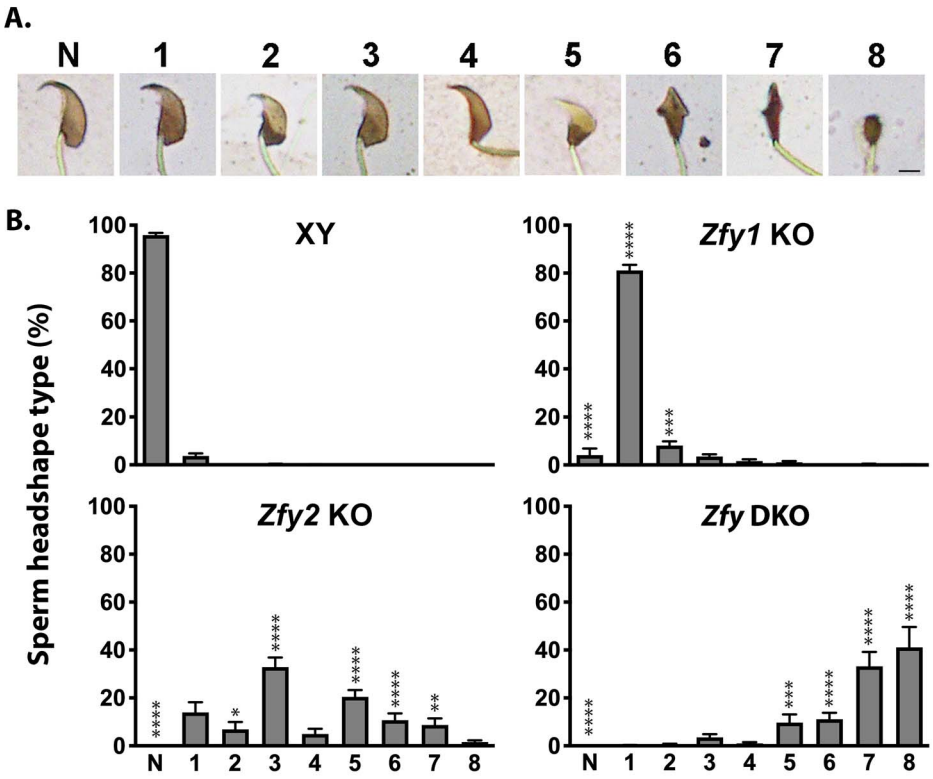

Figure 3. Sperm headshape analysis. (A) The categories of headshape defects. Normal (N): the head has a crescent shape with well-developed acrosome, dorsal and caudal curvature, and a long hook. (1) The crescent shape of head is well maintained with slight flattening of the caudal curvature. The acrosome and hook are well developed and similar to those of normal sperm. (2) The crescent shape of head is still maintained with some flattening in both dorsal and caudal curvature. The acrosome is slightly flattened. The hook is easily recognizable but less pronounced and shorter than in normal sperm. (3) This is a more severe version of type 2. (4) The head is thin and elongated but retains some curvature, and usually a hint of a hooked tip. (5) The head does not have a crescent shape, but some curvature remains. Remnants of the hook and hook tip in most cases are still visible. (6) The head has a rhombus-like shape. Remnants of the hook are no longer visible. (7) This is a more severe version of type 6 with a thinner rhombus-like shape head, no curvature, and no trace of a hook. (8) The head is smaller than any other type and has an egg-like or oval shape with no trace of a hook. Scale = 2.5 μm. (B) The distribution of specific headshape categories among epididymal sperm (~100 sperm examined per male) from control ($n = 12$; 4, 3, and 5 siblings of *Zfy1* KO, *Zfy2* KO and *Zfy* DKO, respectively, carrying an intact Y chromosome), *Zfy1* KO ($n = 8$), *Zfy2* KO ($n = 10$), and *Zfy* DKO ($n = 12$) males. The data were analyzed with ANOVA with genotype (control, *Zfy1* KO, *Zfy2* KO, and *Zfy* DKO) and headshape type (N and 1–8) as factors. Statistically significant effects were observed for genotype, headshape type, and interaction between the two factors ($P < 0.0001$). Post-hoc Bonferroni paired comparison revealed statistically significant differences between specific Headshape Type in control and *Zfy* KO (*$P < 0.05$, **$P < 0.01$; ***$P < 0.001$; ****$P < 0.0001$).

The differences between *Zfy2* KO and *Zfy1* KO are likely due to the quantitative and qualitative differences in expression. Past analyses revealed that *Zfy1*and *Zfy2* are both are expressed primarily in germ cells in the postnatal testis [8, 9]. No expression was detected in Sertoli cells and other somatic cells of the testis with RNA-FISH [18], and our analysis of recent testicular scRNA-seq data [39] also supported negligible expression from Sertoli cells. *Zfy* expression starts at the time when the germ cells enter meiosis, continues until pachytene, at which time both genes undergo MSCI, then both genes are reactivated in the interphase between the two meiotic divisions and continue to be expressed postmeiotically [12, 13, 18]. Premeiotically, *Zfy1* transcripts predominate but most of them are splice variants encoding a protein expected to lack the ability to activate target genes [18]. Postmeiotically, *Zfy2* expression is driven by an "acquired" spermatid-specific promoter derived from an X-linked CYPT gene [7] and is much higher than that of *Zfy1* [18].

Several types of males, with Y chromosome deficiencies and variable *Zfy* contribution, were previously investigated to pinpoint the functional differences between *Zfy1* and *Zfy2* [10–16, 38]. The findings acquired with these mice have shown that early during meiosis, *Zfy1* and *Zfy2* play to some extend overlapping but nevertheless distinct roles [10–12, 38]. However, in later meiotic stages, and postmeiotically, *Zfy2* becomes more functionally significant, with roles in facilitating the 2nd meiotic division [13] and sperm morphogenesis [14, 15]. Based on expression differences, and analyses of prior mouse models, it has been suggested that *Zfy1* plays a dual role in spermatogenesis to produce both activator and repressive proteins while *Zfy2* serves as a super active transcription factor [13].

Here we have shown that *Zfy2* is overexpressed in *Zfy1* KO males. It is possible that this high expression of a super active factor compensates for *Zfy1* loss, justifying lack of spermiogenic phenotype in *Zfy1* KO males. Mild spermiogenic phenotype of *Zfy2* KO males could be explained by insufficiency of retained *Zfy1* transcripts, both in their quantity and functional prowess, to compensate for *Zfy2* loss. It is also entirely possible that the differences originate from functional differences between the two ZFY isoforms.

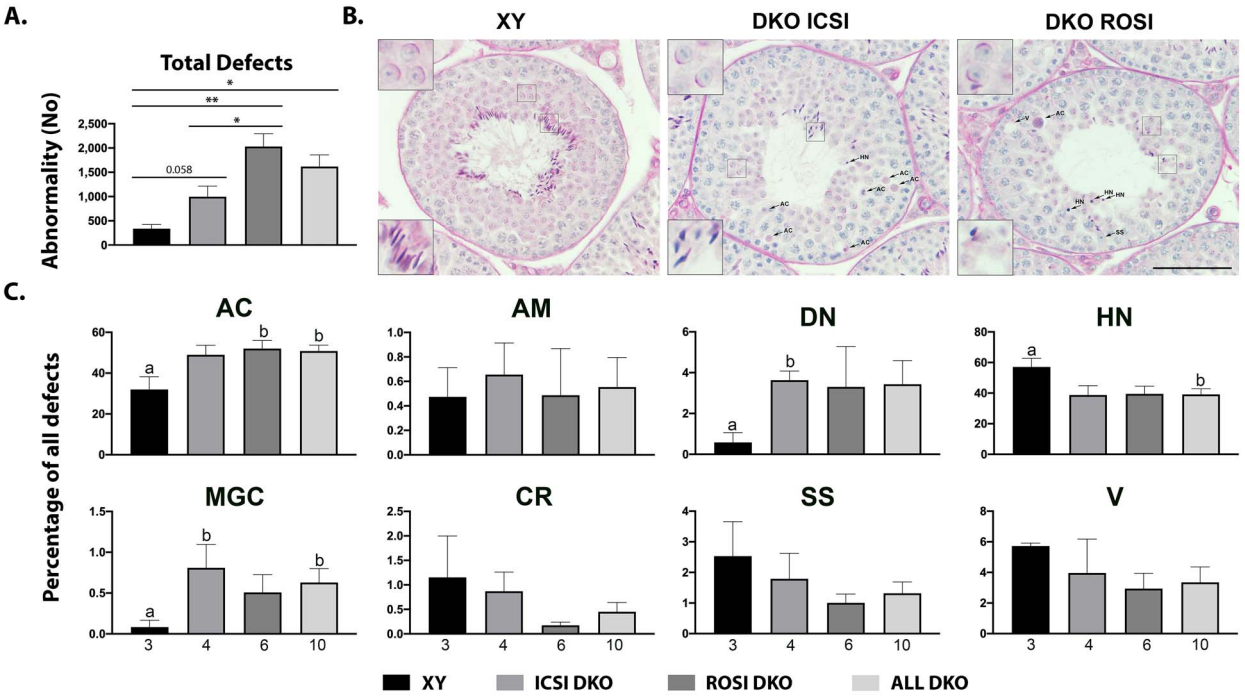

Figure 4. Testis histology. *Zfy* DKO males produced by ICSI (ICSI) and ROSI (ROSI) were compared with with-type control males with intact *Zfy* (XY) regarding a total number of seminiferous epithelium defects. Bars are averages ± SEM. For each male, 60 tubules, 10 of each stage cluster (XII–I, II–IV, V–VI, VII–VIII, IX–X, XI), were scored. Eight cell defect categories were differentiated and counted based on criterial described in [34]: AC, apoptotic cell; AM, apoptotic cell at meiotic metaphase; DN, degenerating nucleus; HN, hypercondensed nucleus; MGC, multinucleated giant cell; CR, cell remnant; SS, sloughed Sertoli cell; V, vacuole. (A) Total number of seminiferous epithelium defects. (B) Exemplary stage VII-VIII tubules of PAS-H-stained sections of testis. DKO ICSI males produced some abnormal elongating spermatids but fewer than XY. DKO ROSI males had postmeiotic arrest and very few abnormal elongating spermatids. Tubules from DKO males often displayed seminiferous defects. Insets show 3× magnification of round spermatids (top) and elongating spermatids (bottom). Scale bar, 100 μm. (C) Frequency of individual cell defect categories. The number of analyzed males is shown under the *x*-axis. Statistical significance (*t*-test): bars marked with different letters are significantly different from each other or as shown in the graph ($^{*}P < 0.05$; $^{**}P < 0.01$).

Consequences of a double *Zfy1* and *Zfy2* gene knockout on spermatogenesis progression and fertility, and sperm quality

Complete loss of *Zfy* genes in *Zfy* DKO males led to infertility and impaired spermatogenesis efficiency with occasional occurrence of a complete postmeiotic arrest and lack of sperm. Spermatogenesis was also not progressing normally, evidenced by increased incidence of seminiferous epithelium defects and morphological and structural changes in round spermatids and epididymal sperm. Because both sperm and round spermatids were functional in assisted fertilization, infertility of *Zfy* DKO males is not due to the deficiency in what sperm contribute to the oocyte. Rather, it reflects either insufficient sperm number or sperm defects that prevents them from fertilizing oocytes on their own.

The severity of postmeiotic arrest in *Zfy* DKO males was inconsistent across generations, with males lacking epididymal sperm yielding sons that produce sperm, and vice-versa, males with sperm yielding sons producing only round spermatids. We reported before a similar leaky postmeiotic arrest with $X^{E}O Sxr^{b}$ males, in which *Zfy* contribution is provided as a *Zfy2/1* fusion gene; in these males, spermatid elongation is initiated but mature sperm are produced rarely [16]. Sperm head defects (abnormal rhombus-like or oval heads lacking curvature and hook, and acrosome defects) observed in *Zfy* DKO males resemble those observed before in males with *Zfy* deficiencies that produce sperm ($X^{E,Z2}Y^{*X}Sry$ males [15]). However, tail structure defects seen here with *Zfy* DKO males, were not reported before [14].

Both *Zfy1* and *Zfy2* are important for normal progression of meiotic divisions [10–16, 38] and males with *Zfy* deficiency were shown before to produce so called "diploid spermatids" (arrested secondary spermatocytes that acquired round spermatid-like morphology) [15, 16, 38]. It was therefore tempting to speculate that decreased spermatid number, presence of abnormal cells in the testis, and sloughed round cells in epididymides in *Zfy* DKO males may be due to spermatid diploidy. Several pieces of evidence go against this theory. We have shown before that round spermatids in $X^{E}O Sxr^{b}$ males elongate and can form sperm. Injection of such sperm to oocytes resulted in ~75% of triploid zygotes, and no offspring could be obtained after ICSI [15]. Here, ICSI with *Zfy* DKO males was successful, and comparable to ROSI outcome. Also, when we performed FACs sorting of spermatogenic cells from *Zfy* DKO male, we were able to obtain decently sized population of haploid round spermatids.

The discrepancies between this study and prior *Zfy* KO and DKO

Our study is a second report on successful *Zfy* gene targeting. In 2017, single and double *Zfy* KO mice were created and characterized by Nakasuji et al. [17]. These authors designed gRNA to target the common sequences in exon 4 of both the *Zfy1* and *Zfy2* genes. Since exon 4 is the differentially

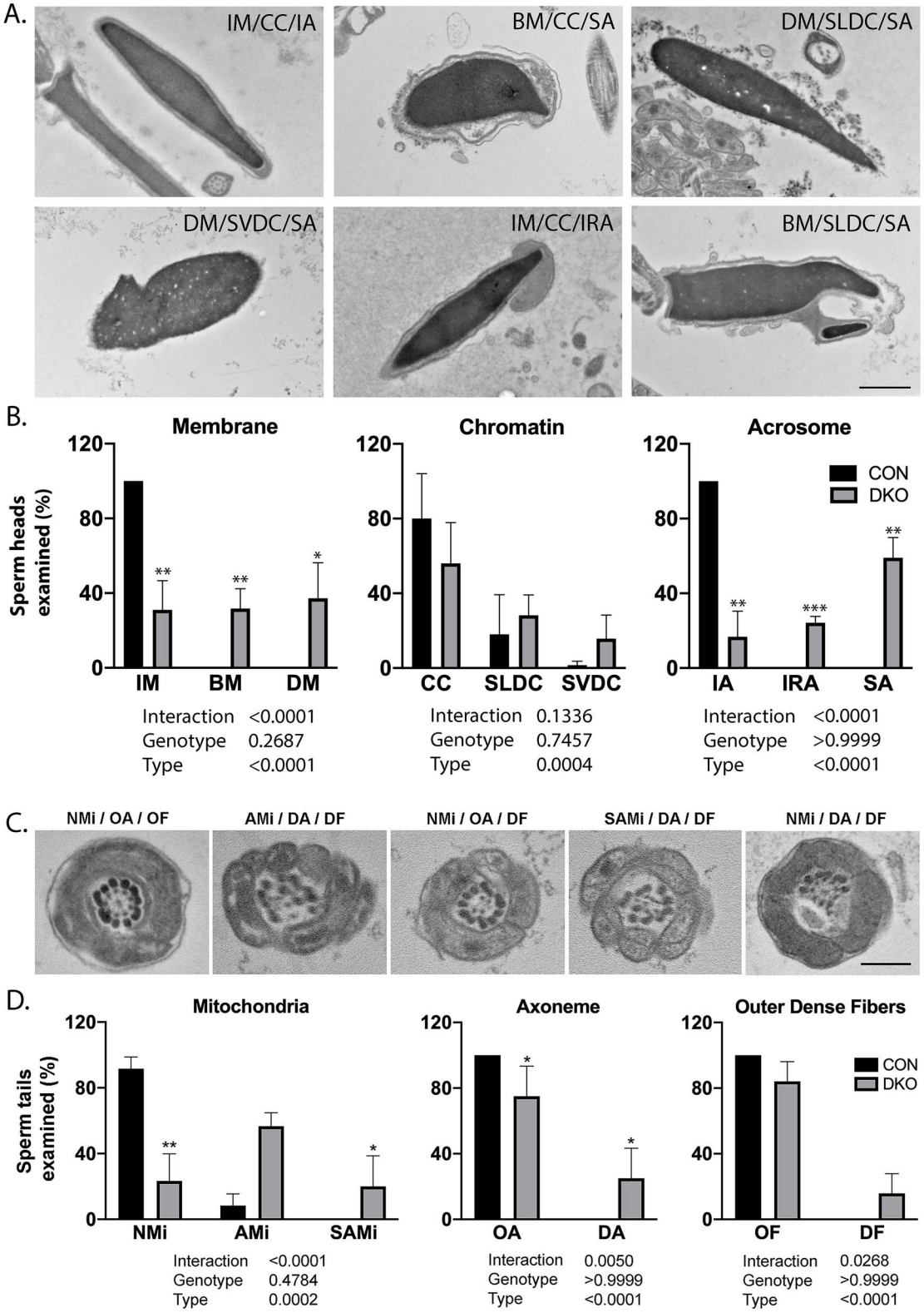

Figure 5. TEM analysis. TEM was used to determine normalcy of head (A and B) and tail (C and D) of sperm from *Zfy* DKO ($n = 4$) and WT control (CON, $n = 2$), with 30 sperm examined per male. Head analyses included assessments of three structures: membrane (IM, intact; BM, broken; DM, disintegrating/ed), chromatin (CC, condensed; SLDC, slightly decondensed; SVDC, severely decondensed), and acrosome (IA, intact; IRA; irregular; SA; separated/not present). (A) Exemplary photos of sperm head defects. Scale, 800 nm. (B) Quantification of membrane, chromatin and acrosome changes. When the data were analyzed with two-way ANOVA with genotype (CON and DKO) and type of structure (IM/BM/DM or CC/SLDC/SVDC or IA/IRA/SA) as factors, no effect of genotype was observed for any of the examined structures. The effect of type was present for all examined structures, and the interaction between two factors was observed for membrane and acrosome but not chromatin. Tail analyses included assessments of three tail structures: mitochondria (NMi, normal; AMi, abnormal; SAMi, severely abnormal), axoneme (OA, organized; DA, disorganized), and outer dense fibers

spliced [18], the targeting strategy allowed for a retention of short transcript variants and consequently retention of some ZFY1 and ZFY2 peptides. The Y genes targeted with CRISPR/Cas9 to date have all been targeted either near the start codon or at a site thought to encode a key domain [17, 40, 41]. Since it is known that following CRISPR/Cas9 editing, transcription through alternative start codons or skipping of mutated/deleted exons can allow functional protein formation [42–45], it is essential to confirm KO at the protein level, or use a strategy that reliably prohibits any protein production. In our study, we removed the entire ORFs of *Zfy1* and *Zfy2* genes, allowing the observed phenotypes to be more confidently assigned to direct (or indirect) consequence of a complete *Zfy* loss.

The comparison of findings from both studies revealed some inconsistencies in phenotypes of KO mice. One would expect that possible retention of ZFY peptides in *Zfy* DKO mice produced by Nakasuji et al. [17] would lead to a milder phenotype than that observed in our work. It is true for some, but not all phenotypic features. Both studies agree that loss of *Zfy2* is more detrimental than loss of *Zfy1*, with decreased litter size and increased incidence of morphologically abnormal sperm in *Zfy2* KO, and not *Zfy1* KO males. However, the spermiogenic phenotype of *Zfy* DKO reported by us here does not fully emulate that reported before by Nakasuji et al. [17]. While we observed decreased testis size and a drastic decrease in sperm number, with some males lacking epididymal sperm entirely, Nakasuji et al. [17] reported that gross appearance of testes and epididymides, testes weights, and sperm numbers were similar for single knockout, double knockout, and WT males. Their qualitative assessment of testis and epididymis cross-sections and immunostaining for markers of sperm structure also did not reveal any impairments. Sperm from *Zfy* DKO males produced by both studies were morphologically abnormal and displayed defects in mitochondria, axoneme, and outer dense fibers. However, while we have not observed defects in sperm motility, Nakasuji et al. [17] observed that sperm from *Zfy* DKO were essentially immotile (1%). Also, while in our hands ICSI and ROSI with haploid gametes from *Zfy* DKO males were successful and efficient, Nakasuji et al. [17] reported that sperm from their DKO males were impaired in their ability to activate oocytes after ICSI, and that embryos after ICSI had chromosome abnormalities and poor developmental potential.

These striking differences in sperm production efficiency and quality and ICSI outcome between Nakasuji et al. [17] and our study are puzzling but also informative and provide clues for future work. Varying genetic background of *Zfy* KO mice (inbred C57BL/6 in our study and hybrid B6D2F2 in Nakasuji et al. [17]) brings a possibility that observed differences in phenotype may be due to genetic background differences and potentially modified by other genes, and thus complex traits rather than monogenic effects. This could be tested in future by exploring consequences of knockout on more genetic backgrounds. Because Nakasuji et al. [17] targeted the differentially spliced exon 4, the knockout was almost certainly selective and removed the long ZFY isoform, which predominates after meiosis and may mediate postmeiotic functions, while leaving the short isoform intact, which predominates prior to meiosis and may be responsible for the earlier functions before/during meiosis. Perhaps retention of the short isoform enabled efficient spermatogenesis and maintenance of normalcy of certain sperm features. Microarray and proteomic analyses of testis and sperm from *Zfy* DKO produced by Nakasuji et al. [17] revealed downregulation of transcripts and proteins of some genes related to reproduction, including those involved with oocyte activation, acrosome reaction, and sperm head maturation. These expression changes fit with their observations regarding sperm behavior in fertilization and ICSI. It is possible that ZFY peptides retained in mice described by Nakasuji et al. [17] led to different dysregulation of expression of *Zfy* target genes than that occurring due to a complete absence of *Zfy* homologues. Future analyses of transcriptome or purified spermatogenic cells and proteome of sperm from our *Zfy* KO models will reveal the consequences of a complete *Zfy* loss, which when related to the previous data [17] may highlight significance of short and long ZFY isoforms.

Conclusions

The mammalian Y chromosome is critical for male sex determination and spermatogenesis, yet linking individual Y genes to specific aspects of male reproduction has been challenging due to inability or limitations of sequences targeting [46]. Here, using mice with a complete loss of *Zfy* genes we explicitly demonstrated that the presence of at least one *Zfy* gene is essential for male fertility in the mouse and that both *Zfy* genes play roles in spermatogenesis. Dissecting the link between *Zfy* genes and key reproductive processes in the mouse enhances understanding of how human ZFY may influence male infertility. The exact mechanism of *Zfy* action remains unknown as previous attempts to obtain specific antibodies for chromatin immunoprecipitation were not successful. The precise targeting strategy of Y chromosome that we applied here can now be adapted to produce epitope-tagged alleles that would pave the way for to future investigations on localization and DNA-binding function of ZFY1 and ZFY2 that would more definitely resolve functional differences between the homologs.

Supplementary material

Supplementary material is available at *BIOLRE* online.

Acknowledgment

Then authors thank Victor Ruthig for consultation regarding testis histology assessment, Wataru Fujii for help with interpretation of gene knockout and preparation of figures showing mutations, Atsushi Sugawara from the Institute for Biogenesis Research Transgenic Core for embryo injections, and Julie Cocquet for helpful comments

Figure 5. (OF, organized; DF; disorganized). (C) Exemplary photos of sperm tail defects. Scale, 400 nm. (D) Quantification of mitochondria, axoneme, and outer dense fibers changes. When the data were analyzed with two-way ANOVA with genotype (CON and DKO) and type of structure (NMi/Ami/SAMi or OA/DA or OF/DF) as factors, no effect of genotype was observed for any of the examined tail structures. The effect of type and the interaction between two factors were significant for all structures. When the frequencies of each type within the same structure were compared between *Zfy* DKO and CON males, statistically significant differences were noted (*t*-test, $^{*}P < 0.05$; $^{**}P < 0.01$). For statistical analyses, percentages were transformed to angles.

on the manuscript draft. The Histology Core at the University of Hawaii was supported by National Institutes of Health (NIH) grant U54MD007601.

Authors' contribution

Y.Y., M.T., J.B., H.H., G.B., and E.C. contributed to data acquisition. M.I. contributed to study conceptualization and design and supervised M.T.; M.A.W. conceptualized and designed the study, acquired funding, contributed to data analysis and data interpretation, administered project, supervised personnel, and wrote a paper. All authors read and approved the manuscript.

Conflict of interest

The authors declare that they have no competing interests.

Data availability

All data generated or analyzed during this study are included in this published article and its supplementary information files.

References

1. Mardon G, Page DC. The sex-determining region of the mouse Y chromosome encodes a protein with a highly acidic domain and 13 zinc fingers. *Cell* 1989; **56**:765–770.
2. Page DC, Mosher R, Simpson EM, Fisher EM, Mardon G, Pollack J, McGillivray B, de la Chapelle A, Brown LG. The sex-determining region of the human Y chromosome encodes a finger protein. *Cell* 1987; **51**:1091–1104.
3. Sinclair AH, Foster JW, Spencer JA, Page DC, Palmer M, Goodfellow PN, Graves JA. Sequences homologous to ZFY, a candidate human sex-determining gene, are autosomal in marsupials. *Nature* 1988; **336**:780–783.
4. Gubbay J, Collignon J, Koopman P, Capel B, Economou A, Munsterberg A, Vivian N, Goodfellow P, Lovell-Badge R. A gene mapping to the sex-determining region of the mouse Y chromosome is a member of a novel family of embryonically expressed genes. *Nature* 1990; **346**:245–250.
5. Koopman P, Gubbay J, Vivian N, Goodfellow P, Lovell-Badge R. Male development of chromosomally female mice transgenic for *Sry*. *Nature* 1991; **351**:117–121.
6. Sinclair AH, Berta P, Palmer MS, Hawkins JR, Griffiths BL, Smith MJ, Foster JW, Frischauf AM, Lovell-Badge R, Goodfellow PN. A gene from the human sex-determining region encodes a protein with homology to a conserved DNA-binding motif. *Nature* 1990; **346**:240–244.
7. Hansen MA, Nielsen JE, Tanaka M, Almstrup K, Skakkebaek NE, Leffers H. Identification and expression profiling of 10 novel spermatid expressed CYPT genes. *Mol Reprod Dev* 2006; **73**: 568–579.
8. Nagamine CM, Chan K, Hake LE, Lau YF. The two candidate testis-determining Y genes (*Zfy-1* and *Zfy-2*) are differentially expressed in fetal and adult mouse tissues. *Genes Dev* 1990; **4**: 63–74.
9. Nagamine CM, Chan KM, Kozak CA, Lau YF. Chromosome mapping and expression of a putative testis-determining gene in mouse. *Science* 1989; **243**:80–83.
10. Royo H, Polikiewicz G, Mahadevaiah SK, Prosser H, Mitchell M, Bradley A, de Rooij DG, Burgoyne PS, Turner JM. Evidence that meiotic sex chromosome inactivation is essential for male fertility. *Curr Biol* 2010; **20**:2117–2123.
11. Vernet N, Mahadevaiah SK, Ojarikre OA, Longepied G, Prosser HM, Bradley A, Mitchell MJ, Burgoyne PS. The Y-encoded gene *zfy2* acts to remove cells with unpaired chromosomes at the first meiotic metaphase in male mice. *Curr Biol* 2011; **21**:787–793.
12. Vernet N, Mahadevaiah SK, de Rooij DG, Burgoyne PS, Ellis PJI. *Zfy* genes are required for efficient meiotic sex chromosome inactivation (MSCI) in spermatocytes. *Hum Mol Genet* 2016; **25**: 5300–5310.
13. Vernet N, Mahadevaiah SK, Yamauchi Y, Decarpentrie F, Mitchell MJ, Ward MA, Burgoyne PS. Mouse Y-linked *Zfy1* and *Zfy2* are expressed during the male-specific interphase between meiosis I and meiosis II and promote the 2nd meiotic division. *PLoS Genet* 2014; **10**:e1004444.
14. Vernet N, Mahadevaiah SK, Decarpentrie F, Longepied G, de Rooij DG, Burgoyne PS, Mitchell MJ. Mouse Y-encoded transcription factor *Zfy2* is essential for sperm head remodelling and sperm tail development. *PLoS One* 2016; **11**:e0145398.
15. Yamauchi Y, Riel JM, Ruthig V, Ward MA. Mouse Y-encoded transcription factor *Zfy2* is essential for sperm formation and function in assisted fertilization. *PLoS Genet* 2015; **11**:e1005476.
16. Yamauchi Y, Riel JM, Stoytcheva Z, Ward MA. Two Y genes can replace the entire Y chromosome for assisted reproduction in the mouse. *Science* 2014; **343**:69–72.
17. Nakasuji T, Ogonuki N, Chiba T, Kato T, Shiozawa K, Yamatoya K, Tanaka H, Kondo T, Miyado K, Miyasaka N, Kubota T, Ogura A *et al.* Complementary critical functions of *Zfy1* and *Zfy2* in mouse spermatogenesis and reproduction. *PLoS Genet* 2017; **13**:e1006578.
18. Decarpentrie F, Vernet N, Mahadevaiah SK, Longepied G, Streichemberger E, Aknin-Seifer I, Ojarikre OA, Burgoyne PS, Metzler-Guillemain C, Mitchell MJ. Human and mouse *ZFY* genes produce a conserved testis-specific transcript encoding a zinc finger protein with a short acidic domain and modified transactivation potential. *Hum Mol Genet* 2012; **21**:2631–2645.
19. Noda T, Sakurai N, Nozawa K, Kobayashi S, Devlin DJ, Matzuk MM, Ikawa M. Nine genes abundantly expressed in the epididymis are not essential for male fecundity in mice. *Andrology* 2019; **7**: 644–653.
20. Naito Y, Hino K, Bono H, Ui-Tei K. CRISPRdirect: software for designing CRISPR/Cas guide RNA with reduced off-target sites. *Bioinformatics* 2015; **31**:1120–1123.
21. Fujihara Y, Kaseda K, Inoue N, Ikawa M, Okabe M. Production of mouse pups from germline transmission-failed knockout chimeras. *Transgenic Res* 2013; **22**:195–200.
22. Noda T, Oji A, Ikawa M. Genome editing in mouse zygotes and embryonic stem cells by introducing SgRNA/Cas9 expressing plasmids. *Methods Mol Biol* 2017; **1630**:67–80.
23. Okabe M, Ikawa M, Kominami K, Nakanishi T, Nishimune Y. "Green mice" as a source of ubiquitous green cells. *FEBS Lett* 1997; **407**:313–319.
24. Nakanishi T, Ikawa M, Yamada S, Parvinen M, Baba T, Nishimune Y, Okabe M. Real-time observation of acrosomal dispersal from mouse sperm using GFP as a marker protein. *FEBS Lett* 1999; **449**: 277–283.
25. Chatot CL, Lewis JL, Torres I, Ziomek CA. Development of 1-cell embryos from different strains of mice in CZB medium. *Biol Reprod* 1990; **42**:432–440.
26. Chatot CL, Ziomek CA, Bavister BD, Lewis JL, Torres I. An improved culture medium supports development of random-bred 1-cell mouse embryos in vitro. *J Reprod Fertil* 1989; **86**:679–688.
27. Riel JM, Yamauchi Y, Ruthig VA, Malinta QU, Blanco M, Moretti C, Cocquet J, Ward MA. Rescue of sly expression is not sufficient to rescue spermiogenic phenotype of mice with deletions of Y chromosome long arm. *Genes (Basel)* 2019; **10**:133.
28. Quinn P. Enhanced results in mouse and human embryo culture using a modified human tubal fluid medium lacking glucose and phosphate. *J Assist Reprod Genet* 1995; **12**:97–105.
29. Nicolson GL, Yanagimachi R, Yanagimachi H. Ultrastructural localization of lectin-binding sites on the zonae pellucidae and plasma membranes of mammalian eggs. *J Cell Biol* 1975; **66**: 263–274.
30. Ward MA, Yanagimachi R. Intracytoplasmic sperm injection in mice. *Cold Spring Harb Protoc* 2018; **2018**:pdb.prot094482.

31. Yamauchi Y, Riel JM, Ruthig VA, Ortega EA, Mitchell MJ, Ward MA. Two genes substitute for the mouse Y chromosome for spermatogenesis and reproduction. *Science* 2016; **351**:514–516.
32. Yamauchi Y, Riel JM, Wong SJ, Ojarikre OA, Burgoyne PS, Ward MA. Live offspring from mice lacking the Y chromosome long arm gene complement. *Biol Reprod* 2009; **81**:353–361.
33. Ahmed EA, de Rooij DG. Staging of mouse seminiferous tubule cross-sections. *Methods Mol Biol* 2009; **558**:263–277.
34. Ruthig VA, Nielsen T, Riel JM, Yamauchi Y, Ortega EA, Salvador Q, Ward MA. Testicular abnormalities in mice with Y chromosome deficiencies. *Biol Reprod* 2017; **96**:694–706.
35. Ward MA, Burgoyne PS. The effects of deletions of the mouse Y chromosome long arm on sperm function–intracytoplasmic sperm injection (ICSI)-based analysis. *Biol Reprod* 2006; **74**:652–658.
36. Brinkworth MH, Weinbauer GF, Schlatt S, Nieschlag E. Identification of male germ cells undergoing apoptosis in adult rats. *J Reprod Fertil* 1995; **105**:25–33.
37. Kanemori Y, Koga Y, Sudo M, Kang W, Kashiwabara S, Ikawa M, Hasuwa H, Nagashima K, Ishikawa Y, Ogonuki N, Ogura A, Baba T. Biogenesis of sperm acrosome is regulated by pre-mRNA alternative splicing of Acrbp in the mouse. *Proc Natl Acad Sci U S A* 2016; **113**:E3696–E3705.
38. Vernet N, Mahadevaiah SK, Ellis PJ, de Rooij DG, Burgoyne PS. Spermatid development in XO male mice with varying Y chromosome short-arm gene content: evidence for a Y gene controlling the initiation of sperm morphogenesis. *Reproduction* 2012; **144**: 433–445.
39. Green KA, Franasiak JM, Werner MD, Tao X, Landis JN, Scott RT Jr, Treff NR. Cumulus cell transcriptome profiling is not predictive of live birth after in vitro fertilization: a paired analysis of euploid sibling blastocysts. *Fertil Steril* 2018; **109**:460.e2–466.e2.
40. Matsumura T, Endo T, Isotani A, Ogawa M, Ikawa M. An azoospermic factor gene, Ddx3y and its paralog, Ddx3x are dispensable in germ cells for male fertility. *J Reprod Dev* 2019; **65**: 121–128.
41. Zuo E, Huo X, Yao X, Hu X, Sun Y, Yin J, He B, Wang X, Shi L, Ping J, Wei Y, Ying W *et al.* CRISPR/Cas9-mediated targeted chromosome elimination. *Genome Biol* 2017; **18**:224.
42. Hosur V, Low BE, Li D, Stafford GA, Kohar V, Shultz LD, Wiles MV. Genes adapt to outsmart gene-targeting strategies in mutant mouse strains by skipping exons to reinitiate transcription and translation. *Genome Biol* 2020; **21**:168.
43. Lindeboom RGH, Vermeulen M, Lehner B, Supek F. The impact of nonsense-mediated mRNA decay on genetic disease, gene editing and cancer immunotherapy. *Nat Genet* 2019; **51**:1645–1651.
44. Sharpe JJ, Cooper TA. Unexpected consequences: exon skipping caused by CRISPR-generated mutations. *Genome Biol* 2017; **18**:109.
45. Smits AH, Ziebell F, Joberty G, Zinn N, Mueller WF, Clauder-Munster S, Eberhard D, Falth Savitski M, Grandi P, Jakob P, Michon AM, Sun H *et al.* Biological plasticity rescues target activity in CRISPR knock outs. *Nat Methods* 2019; **16**:1087–1093.
46. Subrini J, Turner J. Y chromosome functions in mammalian spermatogenesis. *Elife* 2021; **10**. https://doi.org/10.7554/eLife.67345.